DOI: https://doi.org/10.33103/uot.ijccce.23.4.7

A Hybrid Fault Detection and Fault Tolerant Control Based on kNN and NN Approaches for ABS Speed Sensors

Ayad Q. Abdulkareem[1], Abdulrahim Th. Humod[2], Oday A. Ahmed[3]
[1]*Department of Electronic Engineering, University of Diyala, Diyala, Iraq*
[2,3]*Department of Electrical Engineering, University of Technology, Baghdad, Iraq*
[1]*eee.19.04@grad.uotechnology.edu.iq*, [2]*30040@uotechnology.edu.iq*, [3]*30205@uotechnology.edu.iq*

Abstract— *To perform fault tolerance for Anti-lock Braking System (ABS), This paper proposes a hybrid Fault Detection and Fault Tolerant Control (FD-FTC) for ABS speed sensors. It utilizes a Fault Detection (FD) unit and a Data Construction (DC) unit. The first one, the FD unit, is based on a kNN classifier model with 99.9% fault detection accuracy to perform three tasks: early fault detection, fault location diagnosis, and excluding faulty signals from being utilized in further processes. On the other hand, the second one, the DC Unit, is based on two separate neural network models. These models have an MSE of 2.01139e-1 and a R2 of 999880 for the first model and an MSE of 1.12486e-0 and 0.999586 for the second model. They are employed to provide an estimated alternative signal for the ABS speed sensors. These estimated signals are employed to perform two tasks: confirming fault detection declared by the FD model and compensating for the excluded faulty signal to fulfill fault accommodation. Both methods are trained and tested with MATLAB and Simulink. Results demonstrate that the proposed hybrid method has the ability to accurately detect and tolerate sensor faults and fulfill its design purpose, especially during emergency braking.*

Index Terms— *Anti-lock Braking System, Fault Tolerant Control, k-Nearest Neighbour, Neural Networks, Speed Sensor Fault.*

I. INTRODUCTION

Anti-lock Braking System has the ability to greatly improve vehicle safety. It is designed to maximize longitudinal friction force and maintain vehicle maneuverability while preventing the wheels from locking up during hard braking [1]. Relative slip computation accuracy is a key control for ABS, and it is based on the measurements of two speed sensors: vehicle speed and wheel speed sensors [2]. The application of the ABS fault detection and fault-tolerant control (FD-FTC) tool is beneficial to ensure normal braking operation under sensor malfunction or failure.

In recent years, data-driven approaches have been increasingly used for the failure detection of industrial equipment and have had a lot of good results [3], [4], [5], [6], and [7]. Data-driven approaches do not rely on the building of exact or simplified physical models, and they can provide more accurate diagnostic results than traditional methods, which rely on a considerable amount of expert knowledge. Researchers have proposed several data-driven approaches based on machine learning and deep learning to solve fault detection and isolation problems. The development of the ABS speed sensor fault detection method has been presented by [8], where a two-separated model based on neural networks serves analytical redundancy purposes by being utilized to construct an alternative signal for each of the ABS speed sensors. These constructed signals are then utilized in FD-FTC operation. Although all the benefits of the implemented method are effective, a particular drawback arises during fault occurrence; that is, when one of the speed sensor signals is faulty, it will be exposed by examining the residual signal, and a fault occurrence will be stated. At the same time, this faulty signal is also being

Received 28/April/2023; Accepted 17/July/2023
 ISSN (Print) 1811-9212 *ISSN (Online) 2617-3352*

DOI: https://doi.org/10.33103/uot.ijccce.23.4.7

utilized by one of the neural network models to construct an alternative signal for the other sensor; this constructed signal will certainly be inaccurate and lead to the declaration of a false fault occurrence.

To overcome this problem, a pre-diagnosis operation is required for the faulty signal to be isolated before being employed in further processes. Such a diagnosis method was presented in [9], where a kNN-based classifier was employed to classify the ABS speed sensor state between a healthy and faulty state. A kNN classifier is a learning-based approach that uses past or historical input and output information acquired from the system to learn about the process model and then utilizes this knowledge for fault detection in real-time system operation [10][11]. From [9], a kNN classifier presents a good performance among other classifiers. A comparison was carried out among three different classifiers (kNN, SVM, and Decision Tree). These classifiers were trained with the same database. The accuracy presented by each classifier was 61.5, 75, and 99.9 percent for the DT, SVM, and kNN, respectively. However, in spite of that, the kNN presents an excellent advantage over the two other classifiers in detecting the fault within the sensor signals; it's still just performing fault detection without fault effect accommodation mechanisms, which is considered an essential task to fulfill tolerance operation and to maintain safe ABS operation during a faulty state.

This paper presents a hybrid FD-FTC that works to detect and tolerate faults in the ABS speed sensors. It demonstrates the cooperation between two different methods to perform hybrid FD-FTC and increase the safety and reliability of the ABS utilized in most modern ground vehicles. The proposed hybrid FD-FTC utilizes two approaches: The first method is the kNN method, which is employed for early fault detection and isolating faulty signals. The second method aims to confirm the fault detection process and accommodate its effect by providing an alternative signal to compensate for the isolated signal in order to keep system behavior at an accepted normal level.

In the sequel, Section II introduces the proposed system methodology. Section III describes the suggested hybrid FD-FTC method and Section IV presents the conclusion.

II. ABS MODELLING

A straightforward and effective method is utilized to drive the ABS model. This method is called the Quarter Car Model (QCM). *Fig. 1* below describes the QCM-based vehicle dynamics during braking [12].

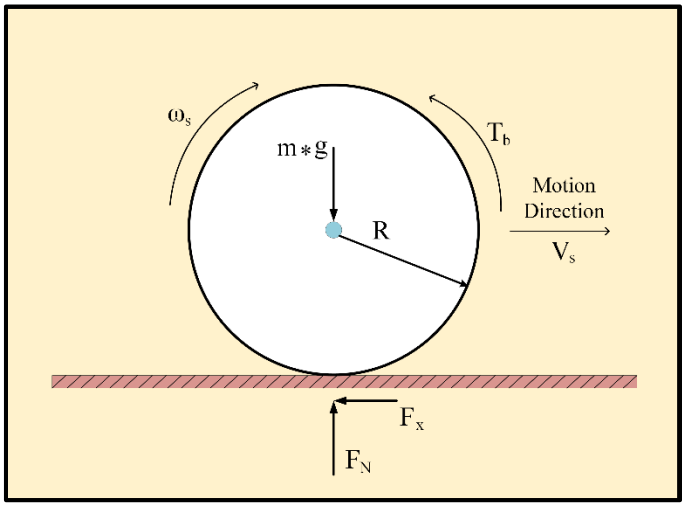

FIG. 1. QCM MODEL [12].

Received 28/April/2023; Accepted 17/July/2023

ISSN (Print) 1811-9212 ISSN (Online) 2617-3352

DOI: https://doi.org/10.33103/uot.ijccce.23.4.7

During braking, the dynamic equation of the deacceleration rotating wheel is [13]:

$$I \times \dot{\omega} = Rr \times F_{fr} - T_b \quad (1)$$

$$\dot{\omega} = \frac{(R_r \times F_{fr}) - T_b}{I} \quad (2)$$

$$\omega = \int \frac{(R_r \times F_{fr}) - T_b}{I} \quad (3)$$

I is the wheel moment inertia, ω rotational wheel speed, R_r is the wheel radius, F_{fr} is the friction force, T_b is the brake torque.

And by Newton's second law of motion, the linear velocity of the vehicle V_s is given by:

$$m \times \dot{V}_s = -F_{fr} \quad (4)$$

$$\dot{V}_s = \frac{-F_x}{m} \quad (5)$$

$$V_s = \int \frac{-F_x}{m} \quad (6)$$

And the calculations of the wheel slip denoted by (λ) performed by [14]:

$$\lambda = \frac{V_s - \omega \times R_r}{V_s} \quad (7)$$

Substitute the equations (3) and (6):

$$\lambda = \frac{\int \frac{-F_x}{m} - \int ((R \times F_x - T_b)/I) * R}{\int \frac{-F_x}{m}} \quad (8)$$

The friction force F_{fr} is calculated by [14]:

$$F_x = m \times g \times \mu(\lambda) \quad (9)$$

Here, the μ is determined by utilizing an empirical model called the Burkhardt model [15]. Burkhardt's model provides an equation that illustrates the nonlinear relation between the friction coefficient and the wheel slip rate for the six standard roads, and it's given below [2]:

$$\mu = C_1\left(1 - e^{C_2 \lambda}\right) - C_3\,\lambda \quad (10)$$

$C_1, C_2, and\ C_3$ are the parameters values for the standard roads [15].

Fig. 2 shows a typical wheel slip - friction coefficient characteristic curve of a tire. It illustrates the variation of the friction coefficient (μ)versus the wheel slip (s) for different road conditions [16].

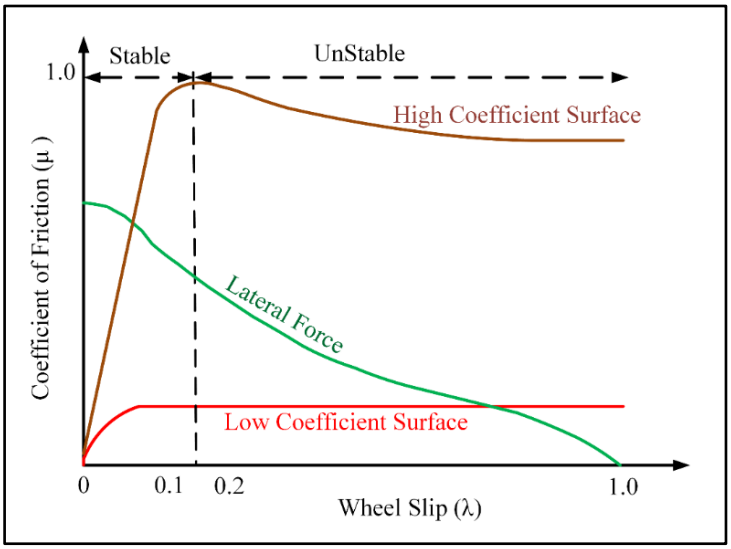

FIG. 2. FRICTION COEFFICIENT (M) VERSUS WHEEL SLIP (S) [16].

Received 28/April/2023; Accepted 17/July/2023

ISSN (Print) 1811-9212 ISSN (Online) 2617-3352

DOI: https://doi.org/10.33103/uot.ijccce.23.4.7

From *Fig. 2*, the value of the wheel slip at which a maximum braking force can be verified is around S = 0.2. So, the ABS has to adjust the applied braking force to keep the slip value at the desired value that leads to efficient braking.

III. PROPOSED HYBRID FD-FTC METHOD

The proposed hybrid FD-FTC method is designed for fault detection and fault tolerant control that may occur in one of the ABS speed sensors in order to maintain safe operation of the ABS, especially during emergency or hard braking.

A. Fault Detection and Diagnosis Unit

This unit employs the kNN, k set equal to 4, classifier algorithm to perform sensor Fault Detection and Diagnosis (FDD) tasks by means of early fault detection, fault location diagnosis and contributes to excluding faulty signals from being utilized in further processes. As illustrated in *Fig. 3*, it receives four input signals: the actual vehicle speed data (V_s_actu), the vehicle speed rate (D_V_s), the actual wheel speed data (ω_s_actu), and the wheel speed rate (D_ω_s). These four signals are evaluated by the kNN algorithm, and based on its training, the algorithm generates an output (kNN decision) that indicates whether a fault is detected on one of the two sensor signals or not.

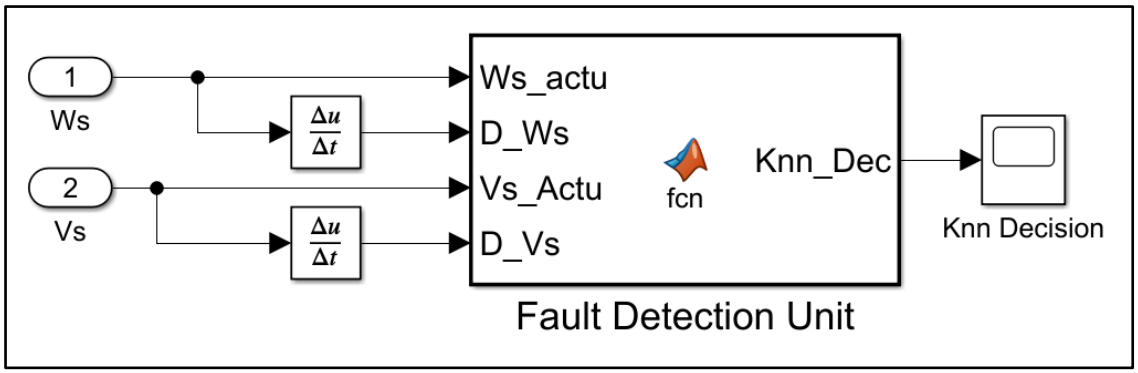

FIG. 3. FAULT DETECTION UNIT PROPOSED IN THIS WORK.

During offline, the training process for the kNN classifier is performed with the MATLAB environment and by adopting the k-neighbors based on distance Euclidean function given by the following equation [17]:

$$d(x,y) = \sqrt{\sum_{i=1}^{n}(x_i - y_i)^2} \quad (11)$$

where x and y are two points with n dimensions. *Fig. 4* illustrates the trained model's testing results.

The trained model is evaluated by two terms, which are sensitivity for each category and overall accuracy. These two terms are calculated using the following equations [9]:

$$Accuracy = \frac{TP+TN}{TP+TN+FN+FP} \quad (12)$$

$$Sensitivity = \frac{TP}{TP+FN} \quad (13)$$

Where:

- True positives (TP): the number of samples that the trained model predicted belonged to a specific class and which actually do belong to that class.
- True negatives (TN) are the number of samples that the trained model predicted do not belong to a specific class but do not actually belong to that class.

Received 28/April/2023; Accepted 17/July/2023

ISSN (Print) 1811-9212 ISSN (Online) 2617-3352

DOI: https://doi.org/10.33103/uot.ijccce.23.4.7

- False positives (FP): the number of samples that the trained model predicted did belong to a specific class but which actually do not belong to that class.
- False negatives (FN) are the number of samples that the trained model predicted did not belong to a specific class but actually did.

Using equation (12), the sensitivities are calculated for the first, second, and third categories, and they are 99.5%, 100.0%, and 98.9%, respectively. This resulted, using equation (13), in an excellent overall accuracy of 99.5%.

A more general dependent classifier test evaluation is performed with two Plots, which are the Confusion Matrix (CM) illustrated in *Fig. 4-A* and the plot of True Positive Rates (TPR) and False Negative Rates (FNR) illustrated in *Fig. 4-B.* From both figures, the trained model showed almost perfect classification ability for the input data samples, with a slight misclassification with respect to the present categories. From the test evaluation, the trained model was considered to have a very good response in distinguishing among different operational conditions and represents a very good choice to serve as an FD method.

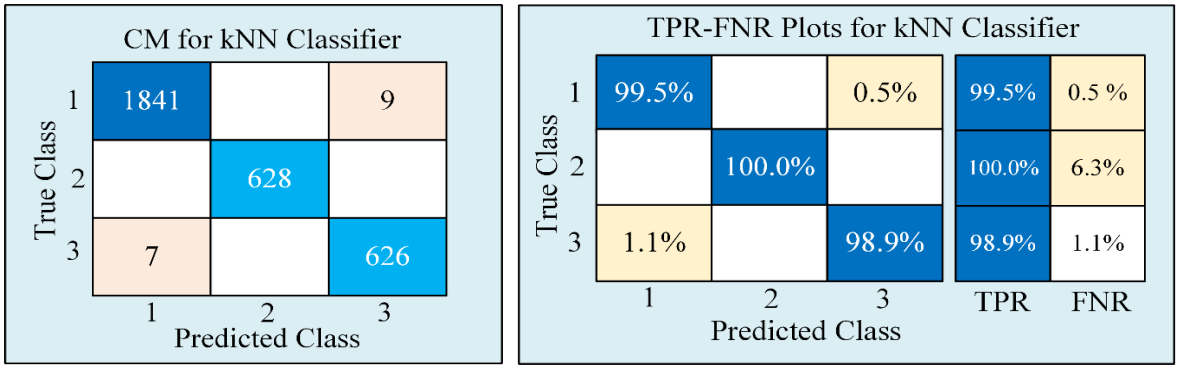

(A) (B)

FIG. 4. KNN MODEL TRAINING RESULTS: (A) CM PLOT., (B) TPR- FNR PLOT.

B. Data Construction Unit

From the perspective of active fault tolerance, a healthy standby signal is required to compensate for the isolated faulty one. These healthy signals can be provided with either hardware or analytical redundancy. In this paper, a MLP-based Neural Network (MLP-NN) aims for fast curve fitting and is utilized to provide an estimated signal for both of the ABS speed sensors to serve as healthy standby signals. The output of MLP-NN first performs the fault detection task by residual signal threshold that confirms the kNN fault detection, and then performs fault effect accommodation by using a compensating the excluded faulty signal.

The MLP-NN receives two signals from the two speed sensors and employs them based on the principle of curve fitting to produce two estimated signals. However, when one of the two speed sensors signals is classified as faulty by the kNN classifier, the estimation operation based on that faulty signal is disabled.

Two MLP network models have been created and trained separately. The Vehicle Speed Estimator (VSE) and Wheel Speed Estimator (WSE) models. The first model is the VSE model, which is utilized to construct or estimate the vehicle speed. Its input layer is formed by the actual wheel speed signal (ω_s) and its rate ($\dot{\omega}_s$), while the output is considered to be the constructed vehicle speed signal ($\widehat{V}_s$). The second model is the WSE model, which is utilized to construct or estimate wheel speed. Its input layer is formed by the actual vehicle speed signal (V_s) and its rate ($\dot{V}_s$). While the output is considered to be the constructed wheel speed signal ($\widehat{\omega_s}$). These two models are identical in their topology, and they differ only in input-output terms. *Fig. 5* shows the topology of the proposed MLP-NN model.

Received 28/April/2023; Accepted 17/July/2023

ISSN (Print) 1811-9212 ISSN (Online) 2617-3352

DOI: https://doi.org/10.33103/uot.ijccce.23.4.7

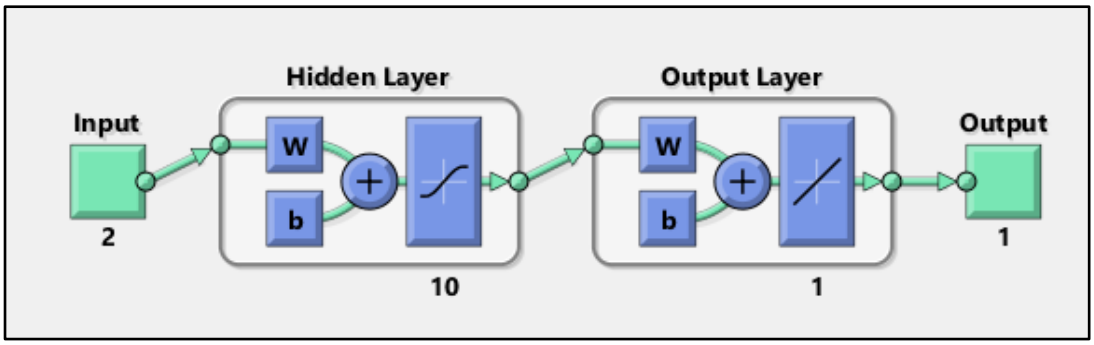

FIG. 5. MLP – NN MODEL TOPOLOGY.

The evaluation operations of both models were evaluated using the MATLAB environment, as their structures are shown in *Fig. 6* and *Fig. 7*, respectively.

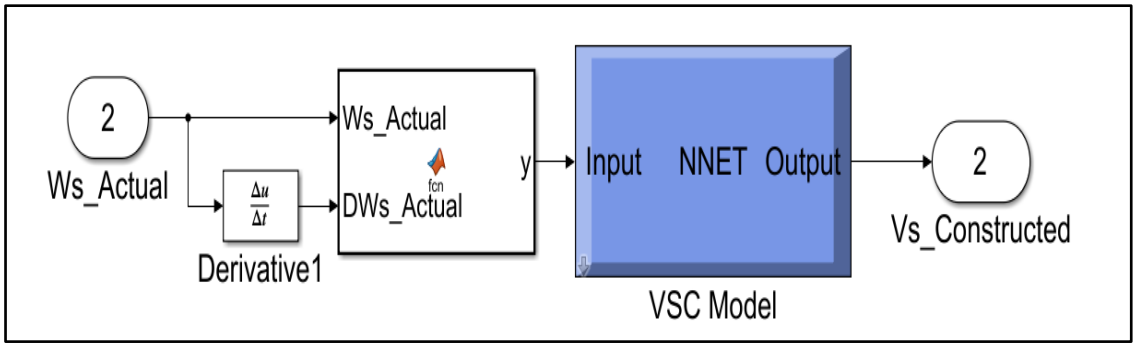

FIG. 6. VSE DATA CONSTRUCTION MODEL STRUCTURE.

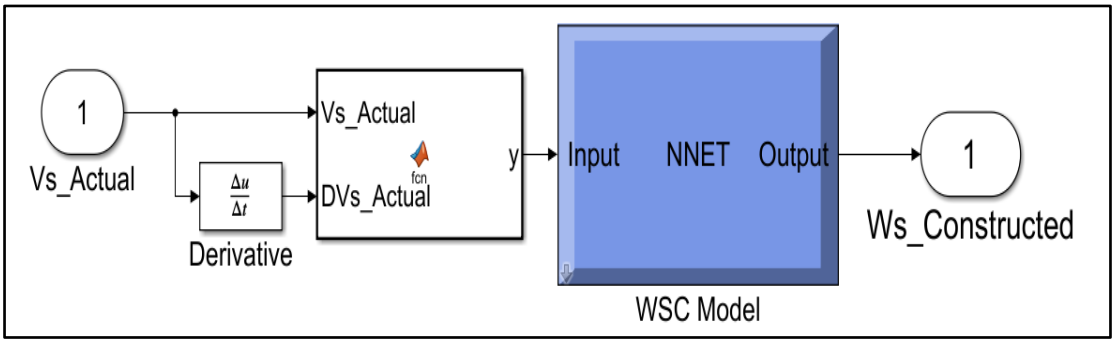

FIG. 7. WSE DATA CONSTRUCTION MODEL STRUCTURE.

The training process was performed with two separate datasets prepared for each model, and each dataset has a total of 17,436 samples. Furthermore, Each dataset has been divided into the following three groups: The first group is 70% (12206 samples) of the dataset and is employed to train the model. The second group is 15% (2615 samples) of the dataset and is employed to train the model validation. The third group is 15% (2615 samples) of the dataset and is employed to train the model for testing purposes. During training, The training data patterns are fed to the network, and the biases and weights values are changed until the error of the training data samples is close to the lowest accepted limit.

Tables I and II demonstrate the performance results for the two models. They display the values of Mean Squared Error (MSE) and the regression coefficient R^2 as related to the three utilized datasets (training, testing, and validation datasets), and it can be seen that both trained models will perform extremely well. as the MSE approaches zero and R^2 approaches unity.

Received 28/April/2023; Accepted 17/July/2023

ISSN (Print) 1811-9212 ISSN (Online) 2617-3352

DOI: https://doi.org/10.33103/uot.ijccce.23.4.7

TABLE I. PERFORMANCE RESULTS OF VSC MODEL

Data Sets	NO. of Samples	MSE	R^2
Training	12206	6.71313e-1	0.999751
Validation	2615	6.36787e-1	0.999759
Testing	2615	1.12486e-0	0.999586

TABLE II. PERFORMANCE RESULTS OF WSC MODEL

Data Sets	NO. of Samples	MSE	R^2
Training	12206	1.90927e-1	0.999894
Validation	2615	2.35444e-1	0.999874
Testing	2615	2.01139e-1	0.999880

C. Reconfiguration Mechanism Unit

This unit is designed to apply certain conditions using the outputs of both the kNN classifier unit output (kNN decision) and the data construction unit output (constructed signals), then perform the required reconfigurations in order to maintain normal operation in a faulty state.

Fig. 8 illustrates the flowchart of the proposed method. The operation procedure performed by it can be described as follows: The acquired data signals from both sensors (V_s and ω_s) are fed to the FDD unit, DC unit, and the reconfiguration unit.

At the FDD unit, these (V_s and ω_s) signals and the corresponding rates of change were examined by the kNN classifier model, and a related classification output signal was generated. This output signal was informed by the kNN decision and was considered a pre-fault detection and diagnosis. The kNN decision signal was fed to the DC unit and reconfiguration unit.

At the DC unit, after receiving data signals (V_s and ω_s) and the kNN decision signal, the kNN decision signal was examined. If this kNN decision indicates a healthy state, then both VSC and VSC models will operate normally and generate the corresponding constructed signals. If the kNN decision belongs to one of the predefined faulty classes, then the DC unit disables one of the developed models that accepts the detected faulty signal as an input signal. In other words, if the faulty signal is the ω_s, then the VSE model will be disabled; if the faulty signal is the V_s, then the WSE model will be disabled.

The disable operation performed by the DC unit is an essential operation because it prevents VSC or WSC models from generating a constructed signal based on a faulty signal. It reveals the important role performed by the kNN classifier. Furthermore, disabled operation is the main reason behind employing the kNN classifier as a fault detection model.

At the reconfiguration unit, after receiving data signals (V_s and ω_s), kNN decision signal, and constructed data signals, the kNN decision signal was examined. If this kNN decision indicates a healthy state, then the actual sensor signals (V_s and ω_s) are passed as output and no modifications are applied. If the kNN decision belongs to one of the predefined faulty classes, then the reconfiguration unit extracts a residual signal by subtracting the constructed signal from the corresponding actual faulty signal. Then, this residual signal is compared to a specified threshold value to confirm the faulty state declared by the FD unit.

After fault occurrence is confirmed, the reconfiguration mechanism performs fault-tolerant operation by adopting the constructed signal provided by the DC unit as a replacement for the faulty detected signal and to be utilized in further system processes, including slip rate calculation.

It's important to mention that, in this thesis, the fault was assumed to occur only on one of the two sensors at a time and not both.

Received 28/April/2023; Accepted 17/July/2023

ISSN (Print) 1811-9212 ISSN (Online) 2617-3352

DOI: https://doi.org/10.33103/uot.ijccce.23.4.7

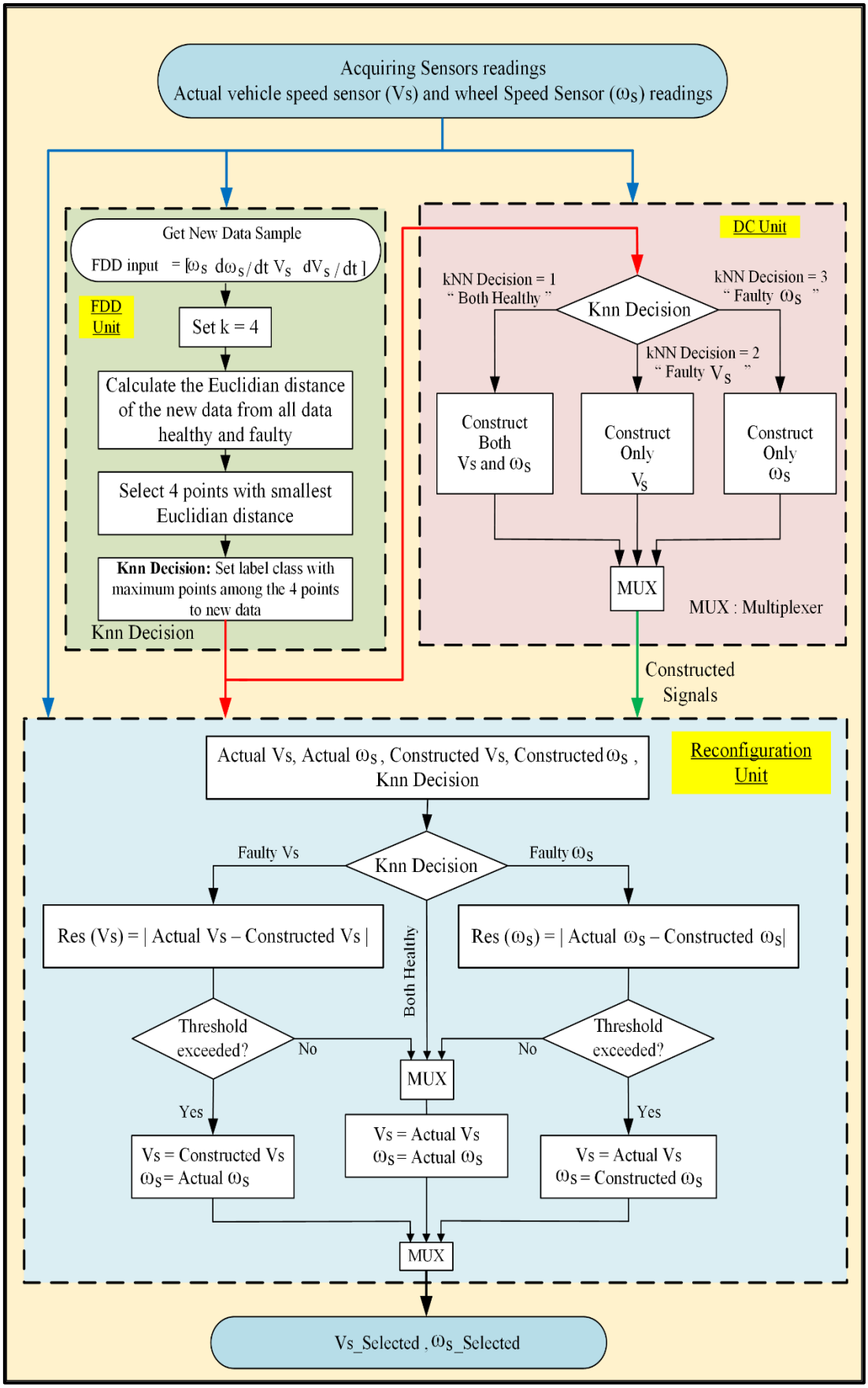

FIG. 8. FLOW CHART OF THE PROPOSED HYBRID METHOD.

Received 28/April/2023; Accepted 17/July/2023

ISSN (Print) 1811-9212 ISSN (Online) 2617-3352

DOI: https://doi.org/10.33103/uot.ijccce.23.4.7

Fig. 9 below shows the ABS model based on quarter-car model implementation in addition to both the proposed models, kNN and data construction models, for online fault detection.

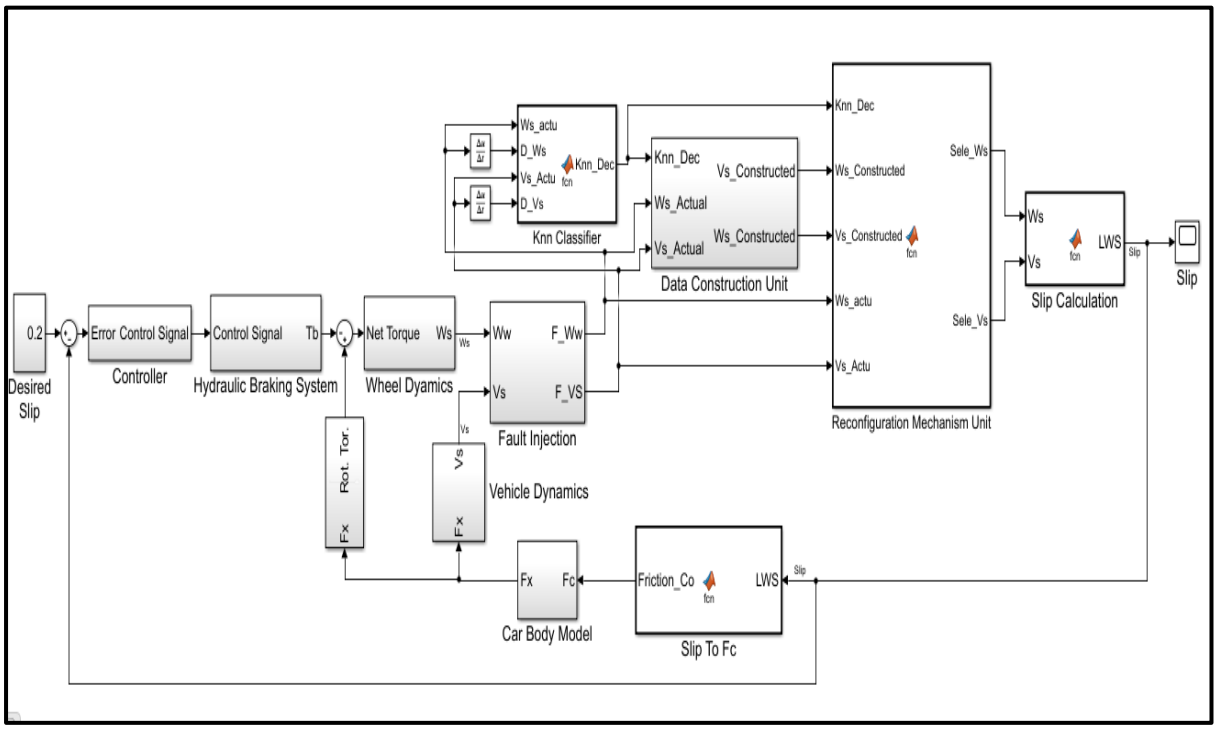

FIG. 9. IMPLEMENTATION OF ABS MODEL WITH THE PROPOSED METHOD.

After the system was implemented, an online performance test was conducted. In the test, the fault was assumed to be in the vehicle speed sensor only; furthermore, the injected faults $(f_1(t)\ and\ f_2(t))$ were assumed to be repeated in different periods of time. Moreover, these $(f_1(t)\ and\ f_2(t))$ are linear and given by the equations below:

$$f_1(t) = \begin{cases} 10t - 20 & 2 \le t \le 3 \\ 40 - 10t & 3 \le t \le 4 \end{cases} \quad (14)$$

$$f_2(t) = \begin{cases} 10t - 60 & 6 \le t \le 7 \\ 80 - 10t & 7 \le t \le 8 \end{cases} \quad (15)$$

Fig. 10 shows the applied faulty signal and the corresponding hybrid FD-FTC response:

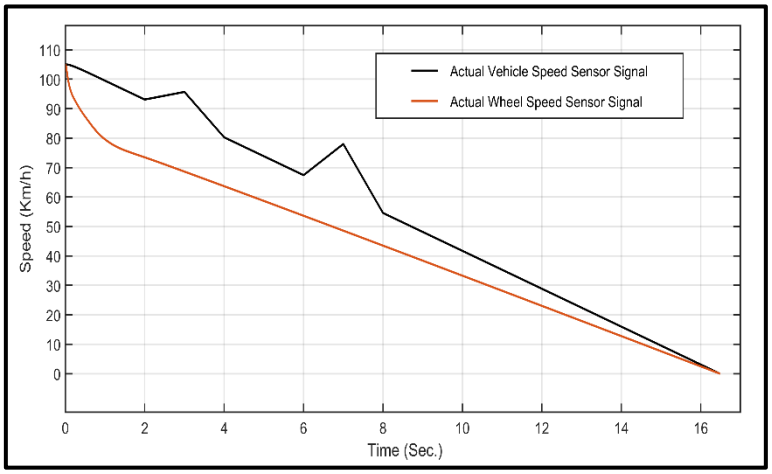

FIG. 10. ACTUAL VEHICLE AND WHEEL SPEED SIGNALS WITH INJECTED FAULTS.

Received 28/April/2023; Accepted 17/July/2023

ISSN (Print) 1811-9212 ISSN (Online) 2617-3352

DOI: https://doi.org/10.33103/uot.ijccce.23.4.7

Regarding the flowchart of the implemented FD-FTC, firstly, the two faulty speed sensor signals with corresponding rates of change were examined by the FD unit that performs a pre-fault detection task. The FDD unit performed examination tasks and generates an output signal called kNN-Decision. And the output signal of the FDD unit displayed in *Fig. 11*.

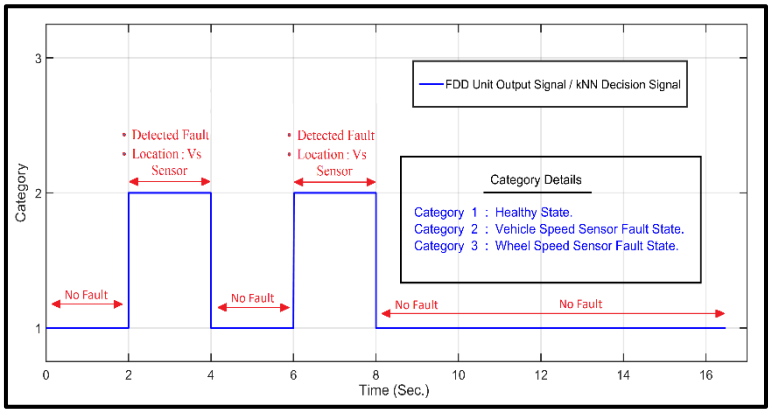

FIG. 11. FDD UNIT OUTPUT (KNN DECISION SIGNAL).

As illustrated in *Fig. 11*. The FDD unit detected and diagnosed two faulty states within the examined two speed signals, and both states fall into category (2), indicating that the fault existed and it was in the vehicle speed sensor.

The FDD unit's output signal and the actual speed sensor signal were received by the DC unit. Then, based on the kNN decision signal, DC unit enabled only the VSC model and employed the wheel speed sensor signal (ω_s_Act.) to construct an alternative signal (V_s_Const.) that corresponds to the faulty detected vehicle speed sensor signal. *Fig. 12* compares the constructed vehicle speed signal (V_s_Const.) with the actual vehicle speed sensor signal (V_s_Act.).

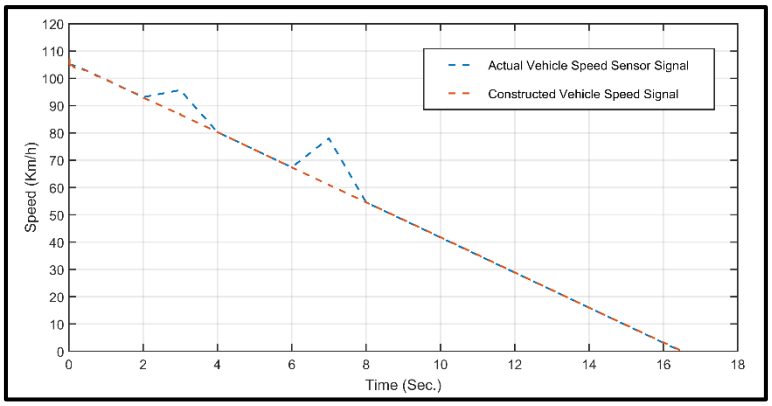

FIG. 12. V_s_CONST. WITH V_s_ACT SIGNALS.

The reconfiguration unit received the actual and constructed signals as well as the kNN decision signal. Based on the kNN decision signal, the reconfiguration unit worked to extract a residual signal, which is the difference between the actual vehicle speed sensor signal and the constructed vehicle speed signal received from the DC unit. *Fig. 13* displays the generated residual signal resulted from subtraction between the actual signal and constructed signals.

Received 28/April/2023; Accepted 17/July/2023

ISSN (Print) 1811-9212 ISSN (Online) 2617-3352

DOI: https://doi.org/10.33103/uot.ijccce.23.4.7

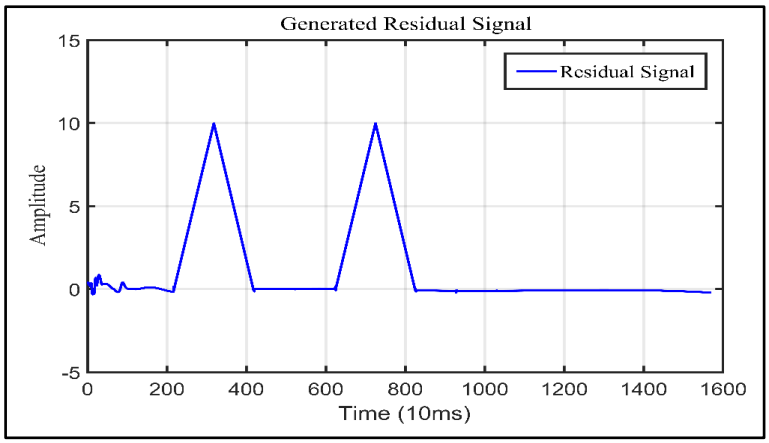

FIG. 13. GENERATED RESIDUAL SIGNAL AT THE RECONFIGURATION UNIT.

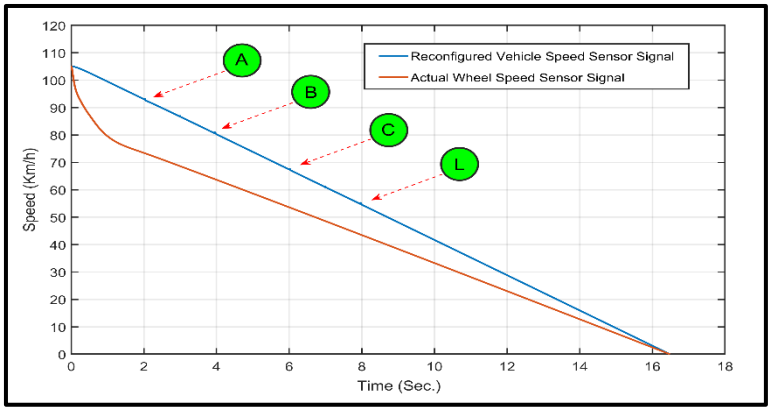

FIG. 14. GENERATED RESIDUAL SIGNAL AT THE RECONFIGURATION UNIT.

The reconfiguration operation was performed for the interval from point (A) to point (B) and from point (C) to point (D). As shown in *Fig. 14*, the faulty part of the signal is isolated and replaced by equavelent healthy part from constructed signal. The output signals of the reconfiguration mechanism unit were used for wheel slip computation. *Fig. 15* displays two wheel slip curve responses: one was calculated using healthy signals, while the other was calculated based on reconfigured signals.

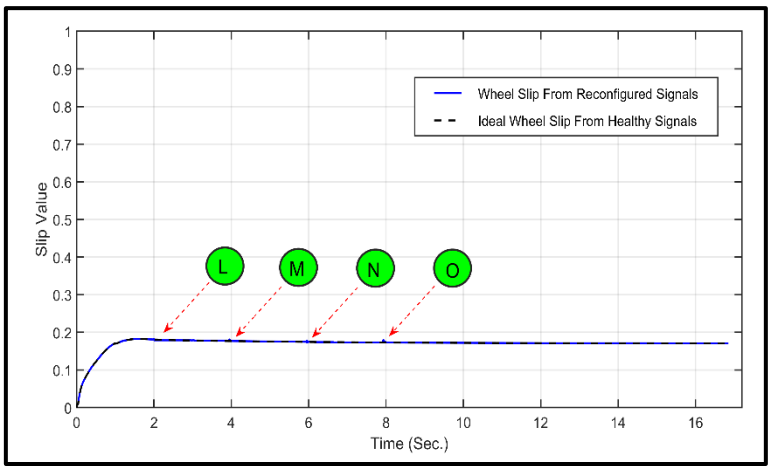

FIG. 15. WHEEL SLIP CURVES - FAULTY STATE AND IDEAL STATE.

As displayed in *Fig. 15*, both signals were similar to each other except that there was a slight trip in the reconfigured slip signal at points L, M, N, and O. This slight trip occurred due to the decision

Received 28/April/2023; Accepted 17/July/2023

ISSN (Print) 1811-9212 *ISSN (Online) 2617-3352*

DOI: https://doi.org/10.33103/uot.ijccce.23.4.7

time taken by the reconfiguration unit to shift from employing the detected faulty signal to employing the responding constructed signal in wheel slip calculation.

From the test results, the implemented method presented stable performance against the injected faults, and the slip wheel was not affected by these faults due to the fault management applied by the implemented hybrid FDD-FTC. Compared to [9], the proposed method presents two advantages. The first one is a higher fault detection accuracy since, beside kNN fault detection, it performs fault detection confirmation through residual signal generation, and the second one is fault effect accommodation or fault tolerance. While, compared to [8], based on the kNN decision signal, it avoids false detection alarms. It utilizes the kNN decision signal to stop signal construction that employs faulty signals.

IV. CONCLUSIONS

To attain a high level of fault detection and fault tolerance, FD-FTC was implemented for ABS speed sensors. The implemented hybrid FD-FTC is based on the cooperation of two models: a kNN classifier with 99.9% fault detection ability and Neural Network models trained to perform fast curve fitting with MSE of 2.01139e-1 and R2 of 999880 for the WSC model and MSE of 1.12486e-0 and 0.999586 for the VSC model. The proposed FD-FTC manages to overcome the previous work's limitations by providing fault tolerance for the detected faults in ABS speed sensors.

Both models were trained and tested in the MATLAB environment, and the result shows that the implemented hybrid method successfully tolerates the occurring sensor faults, fulfilling its design purpose. As a next step for increasing ABS reliability, a hydraulic unit fault tolerance is planned to be implemented.

REFERENCES

[1] L. He, W. Ye, Z. He, K. Song, and Q. Shi, “A combining sliding mode control approach for electric motor anti-lock braking system of battery electric vehicle,” *Control Eng. Pract.*, vol. 102, no. June, 2020, doi: 10.1016/j.conengprac.2020.104520.

[2] Y. Yang, Q. Tang, L. Bolin, and C. Fu, “Dynamic coordinated control for regenerative braking system and anti-lock braking system for electrified vehicles under emergency braking conditions,” *IEEE Access*, vol. 8, pp. 172664–172677, 2020, doi: 10.1109/ACCESS.2020.3024918.

[3] P. Kumar and A. S. Hati, “Review on Machine Learning Algorithm Based Fault Detection in Induction Motors,” *Arch. Comput. Methods Eng.*, vol. 28, no. 3, pp. 1929–1940, 2021, doi: 10.1007/s11831-020-09446-w.

[4] Y. Zhao, T. Li, X. Zhang, and C. Zhang, “Artificial intelligence-based fault detection and diagnosis methods for building energy systems: Advantages, challenges and the future,” *Renew. Sustain. Energy Rev.*, vol. 109, no. April, pp. 85–101, 2019, doi: 10.1016/j.rser.2019.04.021.

[5] L. Gao, D. Li, L. Yao, and Y. Gao, “Sensor drift fault diagnosis for chiller system using deep recurrent canonical correlation analysis and k-nearest neighbor classifier,” *ISA Trans.*, no. xxxx, 2021, doi: 10.1016/j.isatra.2021.04.037.

[6] J. Lu, W. Qian, S. Li, and R. Cui, “Enhanced k-nearest neighbor for intelligent fault diagnosis of rotating machinery,” *Appl. Sci.*, vol. 11, no. 3, pp. 1–15, 2021, doi: 10.3390/app11030919.

[7] A. Mukherjee, P. K. Kundu, and A. Das, “Classification and localization of transmission line faults using curve fitting technique with Principal component analysis features,” *Electr. Eng.*, vol. 103, no. 6, pp. 2929–2944, 2021, doi: 10.1007/s00202-021-01285-7.

[8] A. Abdulkareem, A. Humod, and O. Ahmed, “Fault Detection and Fault Tolerant Control for Anti-lock Braking Systems)ABS) Speed Sensors by Using Neural Networks,” *Eng. Technol. Journal6*, vol. 41, no. 2, pp. 1–12, 2022, doi: 10.30684/etj.2022.135106.1259.

[9] A. Q. Abdulkareem, A. T. Humod, and O. A. Ahmed, “Robust Pattern Recognition Based Fault Detection and Isolation Method for ABS Speed Sensor,” *Int. J. Automot. Technol.*, vol. 23, no. 6, pp. 1747–1754, Dec. 2022, doi: 10.1007/s12239-022-0152-5.

[10] S. Nasser, I. Hashim, and W. Ali, “Visual Depression Diagnosis From Face Based on Various Classification Algorithms,” *Eng. Technol. J.*, vol. 38, no. 11, pp. 1717–1729, 2020, doi: 10.30684/etj.v38i11a.1714.

Received 28/April/2023; Accepted 17/July/2023

 ISSN (Print) 1811-9212 ISSN (Online) 2617-3352

DOI: https://doi.org/10.33103/uot.ijccce.23.4.7

[11] A. Abed, S. Gitaffa, and A. Issa, "Quadratic Support Vector Machine and K-Nearest Neighbor Based Robust Sensor Fault Detection and Isolation," *Eng. Technol. J.*, vol. 39, no. 5A, pp. 859–869, 2021, doi: 10.30684/etj.v39i5a.2002.

[12] D. K. Yadav, "Modeling an intelligent controller for anti-lock braking system," *Int. J. Tech. Res. Appl.*, vol. 3, no. 4, pp. 122–126, 2015.

[13] Y. He, C. Lu, J. Shen, and C. Yuan, "A second-order slip model for constraint backstepping control of antilock braking system based on Burckhardt's model," *Int. J. Model. Simul.*, vol. 40, no. 2, pp. 130–142, 2020, doi: 10.1080/02286203.2019.1570449.

[14] W. Sun, J. Zhang, and Z. Liu, "Two-Time-Scale Redesign for Antilock Braking Systems of Ground Vehicles," *IEEE Trans. Ind. Electron.*, vol. 66, no. 6, pp. 4577–4586, 2019, doi: 10.1109/TIE.2018.2864719.

[15] R. Bhandari, S. Patil, and R. K. Singh, "Surface prediction and control algorithms for anti-lock brake system," *Transp. Res. Part C Emerg. Technol.*, vol. 21, no. 1, pp. 181–195, 2012, doi: 10.1016/j.trc.2011.09.004.

[16] A. Mirzaei, M. Moallem, and B. Mirzaeian, "Designing a genetic-fuzzy anti-lock brake system controller," *Int. J. Eng. Trans. B Appl.*, vol. 18, no. 2, pp. 197–205, 2005.

[17] L. Gao, D. Li, L. Yao, and Y. Gao, "Sensor drift fault diagnosis for chiller system using deep recurrent canonical correlation analysis and k-nearest neighbor classifier," *ISA Trans.*, vol. 122, no. xxxx, pp. 232–246, 2022, doi: 10.1016/j.isatra.2021.04.037.

Received 28/April/2023; Accepted 17/July/2023

 ISSN (Print) 1811-9212 *ISSN (Online) 2617-3352*